

# **Global ENA observations of the storm mainphase ring current: Implications for skewed electric fields in the inner magnetosphere**

P. C:son Brandt<sup>1</sup>, S. Ohtani<sup>1</sup>, D. G. Mitchell<sup>1</sup>, M. -C. Fok<sup>2</sup>, E. C. Roelof<sup>1</sup>, R. Demajistre<sup>1</sup>

Short title: SKEWED MAIN PHASE RING CURRENT

---

<sup>1</sup>The Johns Hopkins University Applied Physics Laboratory, Laurel, MD

<sup>2</sup>NASA Goddard Space Flight Center

**Abstract.** The ring current in the 27-39 keV range during 19 geomagnetic storm main phases is investigated. The data is obtained by the high energy neutral atom (HENA) imager on board IMAGE. Global ion distributions are derived from the observed energetic neutral atom (ENA) images using a constrained linear inversion technique. The peak of the ion distribution is skewed to the midnight to dawn sector, whereas in the classical picture the fluxes peak at dusk. The skewing angle is increasing with the total solar wind electric field across the magnetosphere. We discuss how this morphology implies the existence of strong and skewed equatorial electric fields in the inner magnetosphere. These observations are consistent with observations and kinetic models that self-consistently calculate the electric field produced by the closure of the partial ring current. These observations point to a new understanding of the main phase ring current.

## 1. Introduction

The electric field of the inner magnetosphere is one of the most important features in understanding the development of the storm-time ring current. The magnetospheric electric field was believed to consist of the convective (solar wind induced) dawn to dusk field and the corotational field of the Earth. This produces a potential pattern with its minimum at dusk. Therefore, ions that are transported from the tail region, around to dusk and then out the dayside magnetopause during main phases of geomagnetic storms, were expected to display a peak of the differential flux around dusk.

Comparisons between observations and ring current models with fixed electric field models have implied an offset in local time for the electric field pattern about 2-3 hours [Baumjohann *et al.*, 1985; Kistler *et al.*, 1989; Jordonova *et al.*, 1998; Fok *et al.*, 1996]. Recently, kinetic models have been constructed where the electric field is calculated self consistently, that is, the models calculate the electric field created by the closure of the partial ring current through the ionosphere [Harel *et al.*, 1981; Fok *et al.*, 2001; Ridley and Liemohn, 2001]. The results of these models suggest an eastward skewing of the electric field pattern. Furthermore, electric field measurements by CRESS reveal strong (6 mV/m) electric fields at  $L < 5$ . The high energy neutral atom (HENA) imager on board IMAGE has imaged the ring current in the 10- 200 keV range since May 2000. In all of the storm main phases the peak fluxes have originated from the midnight to dawn sector, consistent with the self-consistent models and the CRESS electric field measurements.

In this paper we present the first global observations of 19 storm main phases that HENA have imaged. We present global ion distributions in the 27-39 keV derived from the observed ENA images through a constrained linear inversion technique [Demajistre *et al.*, 2002; *C:son Brandt et al.*, 2002a]. We show that the local time location of the observed peak in the ion distribution is well correlated with the strength of the solar wind electric field over the magnetosphere. We discuss a possible interpretation of the discrepancy from the expected pattern in light of observations of strong electric fields observed in the inner magnetosphere

and kinetic models.

## 2. Global ring current observations

**Table 1.**

Table 1 lists the times of the storm main phases that are investigated in this paper. In the first three columns we show the times of observation, in the next three we show the IMF  $B_y$ ,  $B_z$  and solar wind velocity  $v_x$  in geocentric solar ecliptic (GSE) coordinates. In the last column we show the local time position of the peak ion flux to within one hour accuracy. The solar wind data has been taken from the ACE space craft and has been lagged for the arrival at Earth. The selected main phases had to fulfil three requirements: (1) The minimum  $Dst \leq -50$  nT for the storm; (2) The main phase had to be at least  $\sim 3$  h long; (3) The IMAGE vantage point had to be close to over the north pole, so that the local time distribution of the ions could be well resolved. During each north-pole passage of the IMAGE space craft, no significant change in the local time distribution could be detected. Each passage offers good viewing over the local time distribution for about 3-6 hours. We stress that the lack of motion of the peak in local time does not imply that the plasma is stagnated. See the Discussion section for a more detailed discussion about the implications.

**Plate 1.**

Plate 1 shows a sample of ion distributions from two main phases. The ion distributions were retrieved from the ENA images by using the constrained linear inversion technique described by *Demajistre et al.* [2002]; *C:son Brandt et al.* [2002a]. This technique assumes a dipolar magnetic field, but since we are focused on the  $L < 5$  ring current we expect no large errors.

**Figure 1.**

We define the skewing angle as the angle between the peak of the ion distribution and local midnight, positive angles in the anti clockwise direction viewed from above the north pole. In Figure 1 we show three plots of the skewing angle as a function of the three quantities for which we found the best correlation coefficients. The first quantity plotted in Figure 1a is the projection of the total IMF in the y-z plane (GSE), i.e.  $B_{tot} = \sqrt{B_y^2 + B_z^2}$ . The second quantity is plotted in Figure 1b is the total solar wind electric field over the magnetosphere,

i.e.  $v_x B_{tot}$ , and the third quantity is the fitting function of the polar cap potential *Weimer* [1995], which can be written as  $v_x B_{tot} \sin(\theta/2)$  where  $\tan \theta = B_y/B_z$ . We see that the correlations are all close to 0.7, which suggests that  $B_{tot}$  is governing the skew for this dataset. The solar wind velocity and the clock angle  $\theta$  appear to only have a minor effect. However, it has to be kept in mind that this dataset is still limited and that no main phases with a strongly negative IMF  $B_y$  has been collected. Therefore, we have to caution the reader to draw any premature conclusions about the (lack of) influence from the solar wind speed and clock angle. Other correlations that were tested includes the IMF  $B_y$ ,  $B_z$ , the epsilon parameter, and the semi-empirical expression for the polar cap potential by *Boyle et al.* [1997], but none of them had a correlation more than 0.54.

### 3. Discussion

Our observations imply some important properties of the electric field. First, the fact that the peak is skewed to the east implies that the electric field is directed such that ions will  $\mathbf{E} \times \mathbf{B}$  drift towards dawn rather than dusk, before the magnetic drift starts dominating and brings the ions duskward. Second, the fact that the local time distribution is concentrated means that the electric potential is localized to the same region. Third, the fact that the same local time distribution is persistent up to 200 keV (not shown here) implies that the electric potential at  $L < 5$  must be deep enough to energize ions to such high energies. This further suggests that the electric fields is strong enough to compete with the magnetic drift. For example, in a 10 mV/m electric field an equatorially mirroring 100 keV proton at  $L=4$  (dipole) will experience an  $\mathbf{E} \times \mathbf{B}$  drift velocity comparable to the magnetic gradient drift velocity.

What causes the eastward skewing of the main phase ion distribution? As was mentioned above, models of the ring current that self-consistently calculates the electric field produced by the closure of the region 2 current system, appears to reproduce this skewing [*Fok et al.*, 2001; *Ridley and Liemohn*, 2001]. Since the conductivity is low in the low-latitude ionosphere where the region 2 currents are believed to close, there will be a substantial potential drop that will

be fed back out to the equatorial magnetosphere. Both the model results and the implications of our observations are supported by observations of unexpectedly strong electric fields in the inner magnetosphere and the low-latitude ionosphere. *Wygant et al.* [1998] reported observations of electric fields during magnetic storms up to 6 mV/m at L=2-4 measured by the CRESS satellite. Fast ionospheric ion flows have been observed by the Millstone Hill Radar facility which implies ionospheric electric field strength 60 mV/m at  $<50^\circ$  MLAT (Personal communication J. Foster, MIT, MA).

The implications of these findings is that a new picture of the build-up of the storm main phase may emerge. The skewed pattern and the significant strength of the magnetospheric electric field at low L-shells may imply that the ion flow during the main phase is brought in to the post midnight sector and exits through the dusk or afternoon magnetopause. There are also indications that this may severely effect how long substorm injections can stay within the magnetosphere [*son Brandt et al.*, 2002b]. A more detailed study is currently being pursued and will be submitted to *J. Geophys. Res.*, .

## References

- Baumjohann, W., G. Haerendel, and F. Melzner, Magnetospheric convection observed between 0600 and 2100 LT: Variations with  $Kp$ , *J. Geophys. Res.*, , *90*, 393–398, 1985.
- Boyle, C. B., P. H. Reiff, and M. R. Hairston, Empirical polar cap potentials, *J. Geophys. Res.*, , *102*, 111–125, 1997.
- C:son Brandt, P., R. Demajistre, E. C. Roelof, D. G. Mitchell, and S. Mende, IMAGE/HENA: Global ENA imaging of the plasmashet and ring current during substorms, *J. Geophys. Res.*, , 2002a, submitted 2002-02-04.
- C:son Brandt, P., D. G. Mitchell, R. Demajistre, E. C. Roelof, S. Ohtani, J.-M. Jahn, C. Pollock, and G. Reeves, Storm-substorm relationships during the 4 october, 2000 storm. image global ena imaging results, *AGU Geophys. Monogr.*, 2002b, submitted 2001-11-30.
- Demajistre, R., E. C. Roelof, P. C:son Brandt, and D. G. Mitchell, Retrieval of global magnetospheric ion distributions from high energy neutral atom (ena) measurements by the image/hena instrument, *J. Geophys. Res.*, , 2002, to be submitted.
- Fok, M. C., T. E. Moore, and M. E. Greenspan, Ring current development during storm main phase, *J. Geophys. Res.*, *101*, 15,311–15,322, 1996.
- Fok, M. C., R. A. Wolf, R. W. Spiro, and T. E. Moore, Comprehensive computational model of Earth's ring current, *J. Geophys. Res.*, , *106*, 8417–8424, 2001.
- Harel, M., R. A. Wolf, P. H. Reiff, R. W. Spiro, W. J. Burke, F. J. Rich, and M. Smiddy, Quantitative simulation of a magnetospheric substorm 1. model logic and overview, *J. Geophys. Res.*, *86*, 2217–2241, 1981.
- Jordonova, V. K., et al., October 1995 magnetic cloud and accompanying storm activity: Ring current evolution, *J. Geophys. Res.*, , *103*, 79–92, 1998.
- Khurana, K. K., R. J. Walker, and T. Ogino, Magnetospheric convection in the presence of

- interplanetary magnetic field  $b_y$ : A conceptual model and simulations, *J. Geophys. Res.*, *101*, 4907–4916, 1996.
- Kistler, L. M., F. M. Ipavich, D. C. Hamilton, G. Gloeckler, B. Wilken, G. Kremser, and W. Stüdemann, Energy spectra of the major ion species in the ring current during geomagnetic storms, *J. Geophys. Res.*, *94*, 3579–3599, 1989.
- Ridley, A. J., and M. W. Liemohn, A model-derived stormtime asymmetric ring current driven electric field description, *J. Geophys. Res.*, , 2001, accepted Aug 2001.
- Weimer, D. R., Models of high-latitude electric potentials derived with a least error fit of spherical harmonic coefficients, *J. Geophys. Res.*, , *100*, 19,595–19,607, 1995.
- White, W. W., G. L. Siscoe, G. M. Erickson, Z. Kaymaz, N. C. Maynard, K. D. Siebert, B. Sonnerup, and D. R. Weimer, The magnetospheric sash and the cross-tail S, *Geophys. Res. Lett.*, , *25*, 1605–1608, 1998.
- Wygant, J., D. Rowland, H. J. Singer, M. Temerin, F. Mozer, and M. K. Hudson, Experimental evidence on the role of the large spatial scale electric field in creating the ring current, *J. Geophys. Res.*, , *103*, 29,527–29,544, 1998.

---

The Johns Hopkins University, Applied Physics Laboratory, 11100 Johns Hopkins Rd.,  
Laurel, MD 20723-6099

Received \_\_\_\_\_

Submitted to *Geophys. Res. Lett.*, 2002-03-18

---

This manuscript was prepared with AGU's  $\text{\LaTeX}$  macros v4, with the extension package 'AGU++' by P. W. Daly, version 1.5f from 1998/07/16.

## Figure Captions

**Plate 1.** Examples of the ion distributions in the 27-39 keV range obtained by inverting the ENA images using a constrained linear inversion technique [*Demajistre et al.*, 2002; *C:son Brandt et al.*, 2002a] for the mainphases of 12 August 2000 and 4 October 2000.

**Figure 1.** Plot showing the correlation between skew angle of the peak ion distribution and the (a) projection of the total IMF onto the y-z GSE plane, (b) total electric field over the magnetosphere, and (c) polar cap potential function by *Weimer* [1995].

## Tables

**Table 1.** Times of observations, solar wind parameters in GSE coordinates and the MLT location of the maximum ion flux.

Year	DOY	UT	$B_y$ (nT)	$B_z$ (nT)	$v_x$ (km/s)	MLT (h)
2000	224	05:00	7	-10	434	04
2000	225	09:40	31	-12	618	05
2000	256	11:00	6	-7	352	23
2000	274	13:53	11	-3	410	01
2000	278	18:00	4	-12	417	03
2000	288	07:40	5	-7	383	02
2000	303	15:00	11	-4	372	00
2000	288	22:56	-5	-5	544	00
2000	358	05:46	5	-11	309	00
2001	078	05:34	-6	-4	300	23
2001	079	10:58	-5	-17	393	00
2001	098	10:35	2	-4	486	22
2001	112	18:30	1	-10	347	23
2001	129	21:57	-2	-8	445	22
2001	275	08:20	1	-5	369	01
2001	275	20:00	0	-7	513	00
2001	276	11:31	1	-20	523	01
2001	294	19:00	25	-8	650	04
2001	305	12:15	10	-6	338	23

## Figures

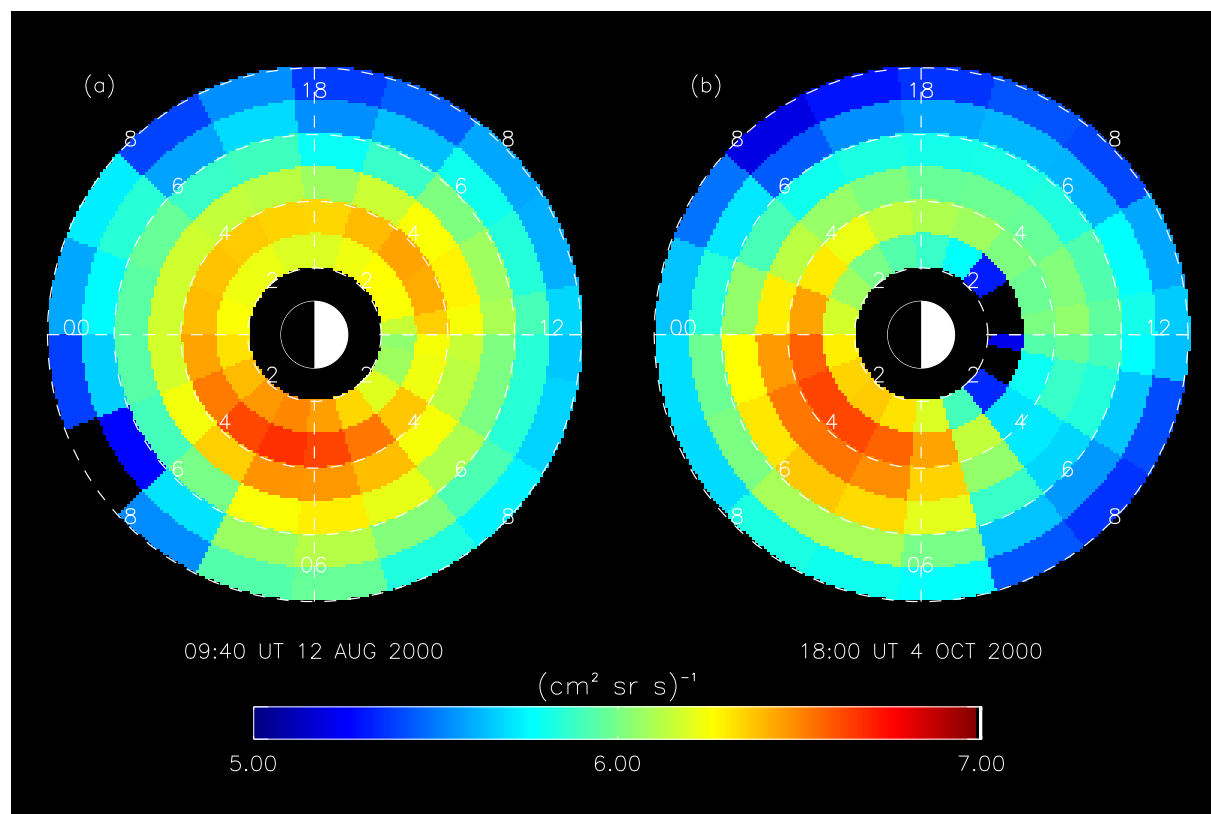


**Plate 1.** Examples of the ion distributions in the 27-39 keV range obtained by inverting the ENA images using a constrained linear inversion technique [Demajstre *et al.*, 2002; *C:son Brandt et al.*, 2002a] for the mainphases of 12 August 2000 and 4 October 2000.

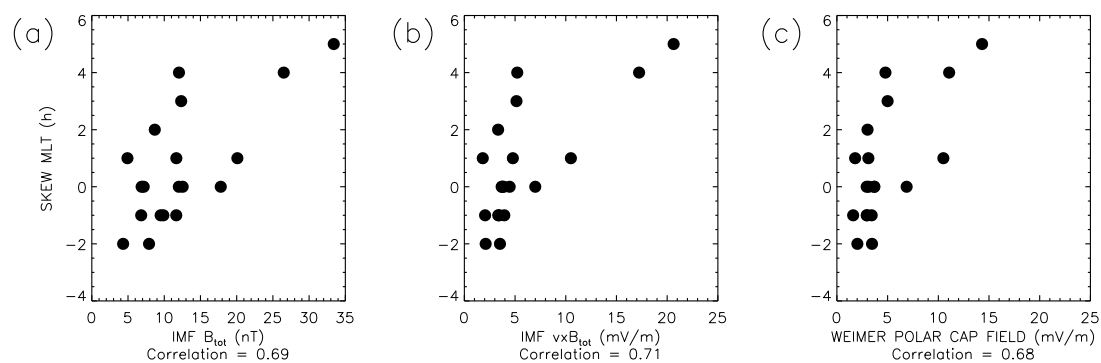


**Figure 1.** Plot showing the correlation between skew angle of the peak ion distribution and the (a) projection of the total IMF onto the y-z GSE plane, (b) total electric field over the magnetosphere, and (c) polar cap potential function by Weimer [1995].